Aggregation Emission Properties of Oligomers Based on Tetraphenylethylene

Weizhi Wang,*,[†] Tingting Lin,[‡] Min Wang,[§] Tian-Xi Liu,[†] Lulu Ren,[†] Dan Chen,[†] and Shu Huang[†]

*Key Laboratory of Molecular Engineering of Polymers of Ministry of Education, Department of Macromolecular Science, Fudan University, Shanghai 200433, Institute of Materials Research and Engineering, A*STAR (Agency for Science, Technology and Research), 3 Research Link, Singapore 117602, and Laboratory of Advanced Materials, Fudan University, Shanghai200438*

Received: November 29, 2009; Revised Manuscript Received: March 30, 2010

A series of eight derivatives based on tetraphenylethylene were prepared, and two of these, i.e., 1,1-bis(4-phenylcarbonyl)-2,2-diphenylethylene (**2**), 1,1,2,2-tetrakis(4-phenylcarbonyl)phenylethylene (**4**), were characterized crystallographically. Because the rigidity and steric hindrance in the molecular structure enhanced regularly from sample **5** to **8**, UV−visible absorption and PL spectra of **5**−**8** show the transition from aggregation-induced emission (AIE) to aggregation-induced emission enhancement (AIEE) behavior. Solid fluorescence lifetime characterization shows that samples with less steric hindrance and more interaction in or between molecules will result in a short fluorescence lifetime. All samples **5**−**8** become more emissive when their chains are induced to aggregate by adding water into their acetonitrile solutions. Cyclic voltammetry measurements taken give the band gap of sample **5**−**8** as 2.88, 2.70, 2.56, and 2.43 eV, and theoretical calculations also support these bad gap results. Conformational simulations also suggest that the origin of transition from AIE to AIEE behavior is due to the restricted intramolecular rotations of the aromatic rings in samples.

Introduction

Tetraphenylethenes (TPE) display interesting chemical and physical properties[1] and can be used as electron transfer catalysts.[2] Furthermore, its rich electrochemical and excited state properties provide excellent research modes for energy transfer.[3] On the other hand, TPE's extended π-systems are also important candidates for incorporation into various organic optoelectronic and optomechanical switching and storage devices,[4] as well as for fluorescent chemosensors.[5]

As novel and unusual phenomena, aggregation-induced emission (AIE),[6,7] and aggregation-induced emission enhancement (AIEE)[8] have recently been given much attention. These findings challenge our current understanding of photoluminescence (PL) processes and aid in deciphering the causes and mechanisms of PL, which may help spawn new photophysical theories and technological innovations. AIE is usually observed in small molecules, such as benzoxazole-based dye by Lee[9] and in organoiridium complexes by Huang.[10] On the other hand, AIEE is only found in polymers and large structure nanoparticles.[8b] Both phenomena are caused by steric interactions in the materials.

One question naturally arises: Can we build steric oligomers to observe the critical change from AIE to AIEE? In this paper, we successfully designed and synthesized tetraphenylethylene derivatives that display this change.

Experimental Section

Materials. Chemicals and reagents were purchased from Aldrich and Acros Chemical Co. unless otherwise stated and used without further purification. All of the solvents were used after purification according to conventional methods when required.

Measurements and Characterization. ^1H and ^{13}C NMR spectra were recorded with Varian Mercury Plus 400 spectrometers, and chemical shifts were reported in ppm units with tetramethylsilane as an internal standard. The UV−visible absorption spectra were obtained in chloroform on a Shimadzu UV-3150 spectrophotometer. The photoluminescence spectra were recorded on a Shimadzu RF-5301 PC fluorometer at room temperature. Lifetime studies were performed with an Edinburgh FL-920 photocounting system with a hydrogen-filled lamp as the excitation source. The data were analyzed by iterative convolution of the luminescence decay profile with the instrument response function using the software package provided by Edinburgh Instruments. The PL quantum yields (Q_F) of the oligomer solutions were measured with 9,10-diphenylanthracene (DPA) in cyclohexane ($Q_F = 90\%$) as the standard. The samples were analyzed by Voyager DE-STR matrix assisted laser desorption-time-of-flight mass spectrometry (MALDI-TOF). Cyclic voltammetry (CV) measurements of the oligomer films coated on a glassy carbon electrode (0.08 cm^2) were performed in an electrolyte of 0.1 M tetrabutylammonium hexafluorophosphate ($TBAPF_6$) in acetonitrile using ferrocene (4.8 eV under vacuum) as the internal standard at a scan rate of 100 mV s^{-1} at room temperature under the protection of argon. A Pt wire was used as the counter electrode and an $Ag/AgNO_3$ electrode was used as the reference electrode. X-ray crystallographic data were collected on a P4 Bruker diffractometer equipped with a Bruker SMART 1K CCD area detector (employing the program SMART) and a rotating anode utilizing graphite-monochromated Mo Kα radiation ($\lambda = 0.710\,73$ Å). Data processing was carried out by use of the program SAINT, while the program SADABS was utilized for the scaling of diffraction data, the application

---

* To whom correspondence should be addressed. Fax: +86 21-65640293. Tel: +86 21-55664180. E-mail: wzwang@ntu.edu.sg.

[†] Department of Macromolecular Science, Fudan University.

[‡] A*STAR.

[§] Laboratory of Advanced Materials, Fudan University.

10.1021/jp911311j

of a decay correction and an empirical absorption correction based on redundant reflections. The structures were solved by using the direct-methods procedure in the Bruker SHELXL program library and refined by full-matrix least-squares methods on F2. All non-hydrogen atoms were refined using anisotropic thermal parameters, and hydrogen atoms were added as fixed contributors at calculated positions, with isotropic thermal parameters based on the carbon atom to which they are bonded.

Theoretical Calculations. All periodic DFT calculations were performed using SIESTA code with numerical-orbital basis sets. The exchange−correlation functional used is the generalized-gradient-approximation method, known as GGA-PBE. A double-ζ plus polarization basis set was employed. The orbital-confining cutoff radii were determined from an energy shift of 0.01 eV. The energy cutoff for the real space grid used to represent the density was set as 150 Ry. To further speed up calculations, Kohn−Sham equation was solved by an iterative parallel diagonalization method that utilizes the ScaLAPACK subroutine pdsygvx with two-dimensional block cyclicly distributed matrix. The accuracy of the SIESTA method was carefully benchmarked with the plane-wave code used previously. The geometry of single molecule (**5**−**8**) was optimized by employing DFT methods at the level of GGA-PW91/DNP (cutoff 3.7 Å) and pseudopotentials available in the DMol^3 module in the Materials Studio Modeling package (Accelrys). The optimization convergences for the energy, force, displacement, and SCF density are 1.0×10^{-5}, 2.0×10^{-3}, 5.0×10^{-3}, and 1.0×10^{-6}, respectively. The HOMO and LUMO were obtained at the optimized structures. Calculations were carried out at $T = 0$ K (DFT), and the gas phase (single molecule) and experimental measurements were done at room temperature and in dilute solutions.

Synthetic Procedures. ***1,1,2,2-Tetraphenylethylene (TPE).*** A solution of diphenylmethane (2.02 g, 12 mmol) in dry tetrahydrofuran (20 mL) was added with 4 mL of a 2.5 M solution of *n*-butyllithium in hexane (10 mmol) at 0 °C under an argon atmosphere. The resulting orange-red solution was stirred for 30 min at that temperature. An appropriate amount of benzophenone (9 mmol) was added to this solution and the reaction mixture was allowed to warm to room temperature with stirring during a 6 h period. The reaction was quenched with the addition of an aqueous solution of ammonium chloride, the organic layer was extracted with dichloromethane (30−50 mL), and the combined organic layers were washed with a saturated brine solution and dried over anhydrous $MgSO_4$. The solvent was evaporated, and the resulting crude alcohol (containing excess diphenylmethane) was subjected to acid-catalyzed dehydration as follows.

The crude alcohol was dissolved in about 80 mL of toluene in a 100 mL Schlenk flask fitted with a Dean−Stark trap. A catalytic amount of *p*-toluenesulfonic acid (342 mg, 1.8 mmol) was added, and the mixture was refluxed for 3−4 h and cooled to room temperature. The toluene layer was washed with 10% aqueous $NaHCO_3$ solution (20−25 mL) and dried over anhydrous magnesium sulfate and evaporated to afford the crude tetraphenylethylene. The crude product was purified by a simple recrystallization from a mixture of dichloromethane and methanol to give a white solid, yield 84%, mp 222−224 °C. ^{1}H NMR ($CDCl_3$, 400 MHz): δ 7.05−7.08 (m, 8H), 7.10−7.13 (m, 12H). ^{13}C NMR ($CDCl_3$, 100 MHz): δ 126.6, 127.8, 131.5, 141.1, 143.9.

1-(4-Phenylcarbonyl)-1,2,2-triphenylethylene (1). To a stirred slurry of 1.33 g (0.01 mol) of aluminum chloride and 3.32 g of TPE (0.01 mol) in 15 mL of CS_2 in room temperature was added, dropwise, a solution of 1.41 g (0.01 mol) of benzoyl chloride in 5 mL of CS_2. When addition was complete, the flask content was reacted for 5 h under room temperature. After that, the reaction mixture was stirred in an ice bath while water was cautiously added. The reaction mixture was extracted with methylene chloride, and the extract was washed with dilute, aqueous sodium hydroxide, dried over magnesium sulfate, and evaporated to give a white solid (3.0 g, 70%). This material was purified by a silica column (petroleum ether:ethyl acetate = 10:1, $R_f = 0.76$), mp 57−58 °C. ^{1}H NMR ($CDCl_3$, 400 MHz): δ 7.20−7.65 (m, 2H), 7.51−7.60 (m, 3H), 7.41−7.47 (m, 2H), 7.08−7.18 (m, 11H), 7.01−7.08 (m, 6H). ^{13}C NMR ($CDCl_3$, 100 MHz): δ 126.9, 127.1, 127.9, 128.1, 128.4, 129.8, 130.1, 131.5, 132.4, 135.4, 138.0, 140.1, 142.8, 143.4, 148.6, 196.5. Anal. Calcd for $C_{33}H_{24}O$ (436.54): C, 90.79; H, 5.54. Found: C, 90.66; H, 5.61. HRMS (MALDI-TOF): *m/z* 436.2 (M^+, 30%), 459.3 ($[M + Na]^+$, 100%).

1,1-Bis(4-phenylcarbonyl)-2,2-diphenylethylene (2). Synthesis steps are the same as for compound **1**: aluminum chloride (2.66 g, 0.02 mol), TPE (3.32 g, 0.01 mol) in 20 mL of CS_2, 2.82 g (0.02 mol) of benzoyl chloride in 5 mL of CS_2, 7 h under room temperature. A green yellow solid (3.1 g, 57%) was purified by silica column (petroleum ether:ethyl acetate = 10:2, $R_f = 0.35$), mp 209−210 °C. ^{1}H NMR ($CDCl_3$, 400 MHz): δ 7.72−7.77 (m, 4H), 7.52−7.62 (m, 6H), 7.42−7.48 (m, 4H), 7.08−7.18 (m, 10H), 7.02−7.08 (m, 4H). ^{13}C NMR ($CDCl_3$, 100 MHz): δ 127.5, 128.1, 128.4, 130.1, 131.5, 132.5, 135.7, 137.8, 139.1, 142.9, 144.4, 147.9, 196.5. Anal. Calcd for $C_{40}H_{28}O_2$ (540.65): C, 88.86; H, 5.22. Found: C, 88.80; H, 5.41. HRMS (MALDI-TOF): *m/z* 539.8 (M^+, 100%), 562.8 ($[M + Na]^+$, 55%).

1,1,2-Bis(4-phenylcarbonyl)-2-phenylethylene (3). Synthesis steps are the same as for compound **1**: aluminum chloride (7.98 g, 0.06 mol), TPE (3.32 g, 0.01 mol) in 50 mL of nitrobenzene, benzoyl chloride (8.46 g, 0.06 mol) of in 10 mL of nitrobenzene, 12 h under 80 °C. A yellow solid (2.97 g, 46%) was purified by silica column (petroleum ether:ethyl acetate = 10:4, $R_f = 0.62$), mp 140−141 °C. ^{1}H NMR ($CDCl_3$, 400 MHz): δ 7.72−7.78 (m, 6H), 7.52−7.64 (m, 9H), 7.42−7.49 (m, 6H), 7.12−7.21 (m, 9H), 7.05−7.10 (m, 2H). ^{13}C NMR ($CDCl_3$, 100 MHz): δ 127.8, 128.5, 130.1, 131.4, 132.6, 136.0, 136.3, 137.7, 140.6, 142.3, 143.2, 147.2, 147.3, 196.3. Anal. Calcd for $C_{47}H_{32}O_3$ (644.76): C, 87.55; H, 5.00. Found: C, 87.51; H, 5.11. HRMS (MALDI-TOF): *m/z* 643.3 (M^+, 100%), 666.3 ($[M + Na]^+$, 90%).

1,1,2,2-Tetrakis(4-phenylcarbonyl)phenylethylene (4). Synthesis steps are the same as for compound **1**: aluminum chloride (13.3 g, 0.1 mol), TPE (3.32 g, 0.01 mol) in 50 mL of nitrobenzene, benzoyl chloride (14.1 g, 0.1 mol) in 10 mL of nitrobenzene, 15 h under 100 °C. A light yellow solid (4.1 g, 55%) was purified by silica column (petroleum ether:ethyl acetate = 10:4, $R_f = 0.30$), mp 233−234 °C. ^{1}H NMR ($CDCl_3$, 400 MHz): δ 7.71−7.77 (m, 8H), 7.60−7.64 (m, 8H), 7.54−7.60 (m, 4H), 7.43−7.49 (m, 8H), 7.17−7.22 (m, 8H). ^{13}C NMR ($CDCl_3$, 100 MHz): δ 128.5, 130.1, 131.4, 132.7, 136.5, 137.6, 142.1, 146.7, 196.2. Anal. Calcd for $C_{54}H_{36}O_4$ (748.86): C, 86.61; H, 4.85. Found: C, 86.49; H, 4.92. HRMS (MALDI-TOF): *m/z* 748.3 (M^+, 40%), 771.3 ($[M + Na]^+$, 100%).

1,4-Bis(1,2,2-triphenylvinyl)benzene (5). To a solution of diphenylmethane (2.02 g, 12 mmol) in dry tetrahydrofuran (20 mL) was added 4 mL of a 2.5 M solution of *n*-butyllithium in hexane (10 mmol) at 0 °C under an argon atmosphere. The resulting orange-red solution was stirred for 30 min at that temperature. To this solution was added an appropriate amount of compound **1** (9 mmol), and the reaction mixture was allowed to warm to room temperature with stirring over a 6 h period. The reaction was quenched with the addition of an aqueous solution of ammonium chloride, the organic layer was extracted with dichloromethane (30−50 mL), and the combined organic layers were washed with a saturated brine solution and dried over anhydrous $MgSO_4$. The solvent was evaporated, and the resulting crude alcohol (containing excess diphenylmethane) was subjected to acid-catalyzed dehydration as follows.

The crude alcohol was dissolved in about 80 mL of toluene in a 100 mL Schlenk flask fitted with a Dean−Stark trap. A catalytic amount of *p*-toluenesulfonic acid (342 mg, 1.8 mmol) was added, and the mixture was refluxed for 3−4 h and cooled to room temperature. The toluene layer was washed with 10% aqueous $NaHCO_3$ solution (20−25 mL), dried over anhydrous magnesium sulfate, and evaporated to afford the crude **5** (5.2 g, 99%). The crude product was purified by a simple recrystallization from a mixture of dichloromethane and methanol, mp 250−251 °C. ^{1}H NMR ($CDCl_3$, 400 MHz): δ 7.08−7.14 (m, 4H), 7.02−7.08 (m, 12H), 6.95−7.02 (m, 12H), 6.73−6.77 (m, 6H). ^{13}C NMR ($CDCl_3$, 100 MHz): δ 126.6, 127.8, 130.9, 131.6, 141.0, 142.0, 143.7, 144.0. Anal. Calcd for $C_{46}H_{34}$ (586.76): C, 94.16; H, 5.84. Found: C, 93.89; H, 6.11. HRMS (MALDI-TOF): *m/z* 586.5 (M^+, 40%), 693.4 ($[M + Ag]^+$, 68%).

1-(2,2-Diphenyl-1-(4-(1,2,2-triphenylvinyl)phenyl)vinyl)-4-(1,2,2-triphenylvinyl)benzene (6). Steps are the same as for compound **5**: diphenylmethane (2.02 g, 12 mmol) in 20 mL of dry tetrahydrofuran, 4 mL of *n*-butyllithium in hexane (2.5 M, 10 mmol), 0 °C, 30 min. After that, compound **2** (4.5 mmol) was added and reacted for 6 h to get crude **6** (3.7 g, 100%). The crude product was purified by a simple recrystallization from a mixture of dichloromethane and methanol. ^{1}H NMR ($CDCl_3$, 400 MHz): δ 7.08−7.11 (m, 8H), 7.06−7.08 (m, 16H), 6.93−7.00 (m, 16H), 6.69−6.74 (m, 8H). ^{13}C NMR ($CDCl_3$, 100 MHz): δ 126.6, 127.7, 128.3, 128.8, 130.7, 130.9, 131.6, 133.1 140.9, 140.1, 141.9, 142.1, 143.8, 144.0. Anal. Calcd for $C_{66}H_{48}$ (841.09): calcd. C 94.25, H 5.75, found C 94.20, H 5.80. HRMS (MALDI-TOF): *m/z* 840.4 (M^+, 30%), 948.3 ($[M+Ag]^+$, 100%).

1-(2-Phenyl-1,2-bis(4-(1,2,2-triphenylvinyl)phenyl)vinyl)-4-(1,2,2-triphenylvinyl)benzene. (7). Steps are the same as for compound **5**: diphenylmethane (2.02 g, 12 mmol) in 20 mL of dry tetrahydrofuran, 4 mL of *n*-butyllithium in hexane (2.5 M, 10 mmol), 0 °C, 30 min. The following steps are same as above to get crude **7** (3.2 g, 100%). The crude product was purified by a simple recrystallization from a mixture of dichloromethane and methanol. ^{1}H NMR ($CDCl_3$, 400 MHz): δ 7.09−7.18 (m, 12H), 7.01−7.09 (m, 20H), 6.91−7.01 (m, 20H), 6.64−6.86 (m, 10H). ^{13}C NMR ($CDCl_3$, 100 MHz): δ 126.7, 127.7, 130.6, 131.0, 131.6, 140.7, 141.7, 142.1, 142.4, 143.9, 144.1. Anal. Calcd for $C_{86}H_{62}$ (1095.41): C, 94.30; H, 5.70. Found: C, 94.32; H, 5.68. HRMS (MALDI-TOF): *m/z* 1094.6 (M^+, 32%), 1203.5 ($[M + Ag]^+$, 100%).

1,1,2,2-Tetrakis(4-(1,2,2-triphenylvinyl)phenyl)ethene (8). Steps are the same as for compound **5**: diphenylmethane (2.02 g, 12 mmol) in 20 mL of dry tetrahydrofuran, 4 mL of *n*-butyllithium in hexane (2.5 M, 10 mmol), 0 °C, 30 min. After that, compound **4** (2.3 mmol) was added and reacted for 6 h to get crude **8** (3.1 g, 100%). The crude product was purified by a simple recrystallization from a mixture of dichloromethane and methanol. ^{1}H NMR ($CDCl_3$, 400 MHz): δ 7.07−7.15 (m, 28H), 6.98−7.07 (m, 24H), 6.90−6.94 (m, 8H), 6.71−6.76 (m, 8H), 6.61−6.66 (m, 8H). ^{13}C NMR ($CDCl_3$, 100 MHz): δ 126.7, 127.8, 130.7, 131.0, 131.7, 140.6, 141.1, 142.0, 142.2, 143.8. Anal. Calcd for $C_{106}H_{76}$ (1349.74): C, 94.32; H, 5.68. Found: C, 94.31; H, 5.69. HRMS (MALDI-TOF): *m/z* 1350.0 (M^+, 100%), 1458.0 ($[M + Ag]^+$, 95%).

SCHEME 1: Synthesis of TPE Derivatives

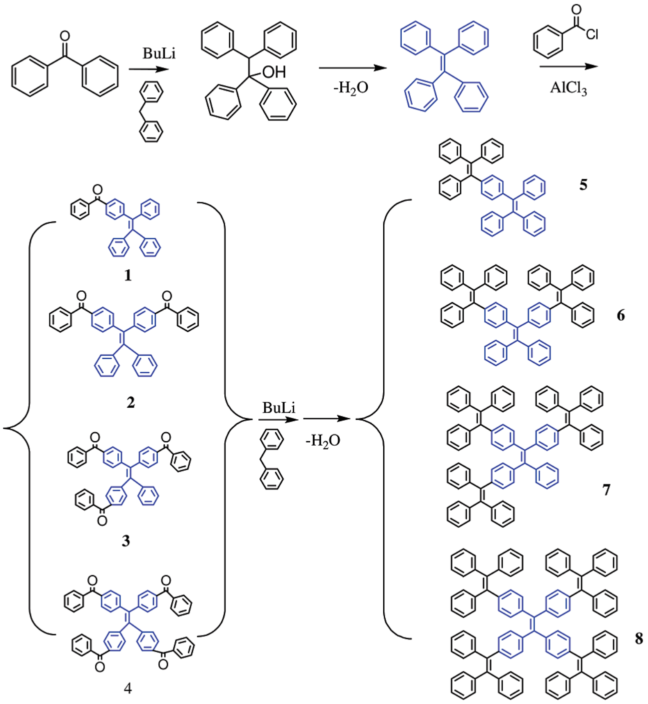

Results and Discussion

Synthesis. Symmetrical TPE are easily prepared via McMurry coupling[11] of the corresponding benzophenones, catalyzed by low-valent titanium. However, it is difficult to prepare unsymmetrical tetraarylethylenes in high yield, even when one of the components is used in sacrificial excess. Using two different benzophenones, the McMurry reaction will produce a mixture of symmetrical and unsymmetrical products. Rathore et al. have recently reported[12] a new method involving dehydration of the corresponding alcohols to afford the unsymmetrical products in nearly quantitative yield. This method is used here to synthesize the tetraphenylethene derivatives **5**−**8** listed in Scheme 1.

The details of reaction of TPE with benzoyl chloride are listed in Table S1 (Supporting Information). It was noticed that when the Lewis acid was added to the reaction mixture containing TPE and the acylating agent in nitrobenzene with the mole ratio 1:4:4 (TPE/benzoyl chloride/$AlCl_3$), a strong dark violet color change occurred for the aluminum chloride and the product forms complexes. It is noteworthy that the desired products **1**, **2**, **3**, and **4** can be synthesized in one step. However, the low yields and difficult separation make it unacceptable. As shown for entries 2, 3, 4, and 5 in Table S1 (Supporting Information), the separated four steps with different TPE/benzoyl chloride/$AlCl_3$ mole ratios can obtain good yield. Most importantly, the separation process can be easily realized. If the solvent was changed to CS_2, the results of products **1** and **2** are better because the solvent can be easily discarded by vacuum.

Friedel−Crafts-type acylation of TPE in the presence of a Lewis acid ($AlCl_3$) gave four differently substituted aromatic products (**1**, **2**, **3**, and **4**) readily in high yield. This electrophilic aromatic substitution allows the synthesis of monoacylated

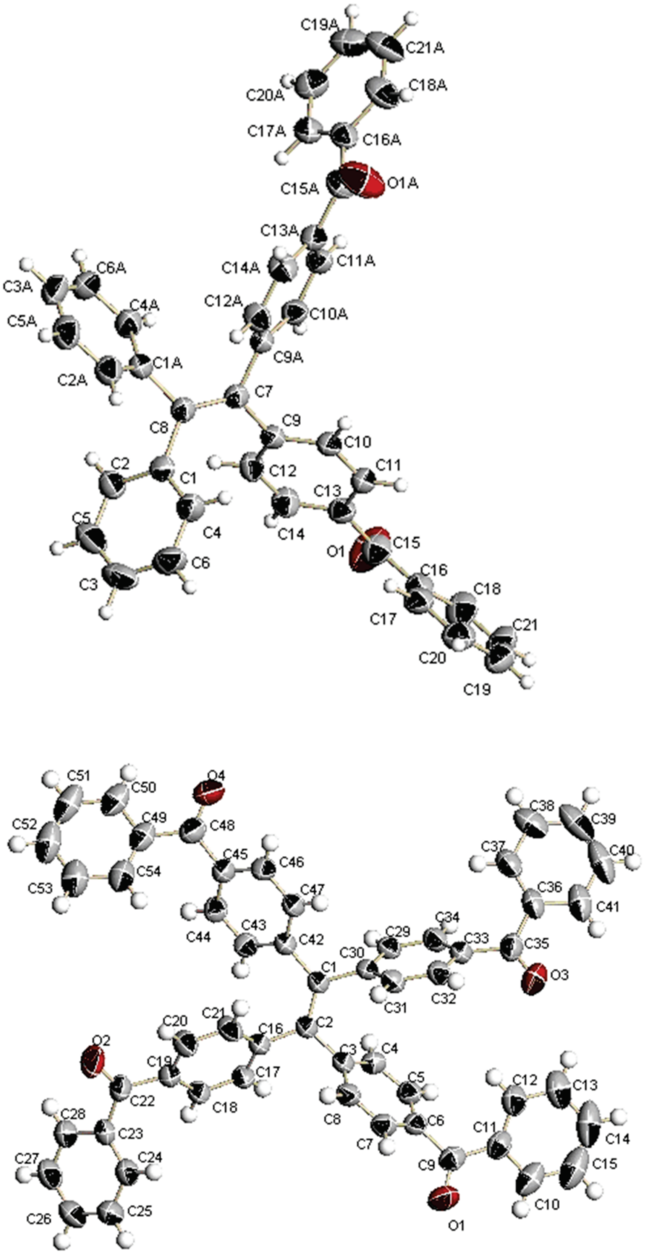

Figure 1. ORTEP drawing of **2** and **4**. The ellipsoid probability is 30%.[13]

products between a benzene ring of TPE and different acyl chlorides. The acylated benzene is deactivated and does not undergo a second substitution. Further acylation only occurs on other benzene rings in TPE. The products are controlled by changing the TPE/benzoyl chloride/$AlCl_3$ molar ratios and reaction conditions. As an example, the structures of **2** and **4** were characterized by X-ray crystallographic analysis in Figure 1 and ref 13.

Optical Properties. To investigate the transition between AIE and AIEE, UV−visible absorption and PL spectra of solutions of **5**−**8** were obtained (Figure 2a). Absorption peaks of **5**−**8** were observed at 313, 320, 328, and 331 nm, respectively. However, the corresponding PL spectra of the solutions were different. **5** and **6** are practically nonluminescent in dilute THF solution. The PL curves of **7** and **8** had maxima at 406 and 462 nm, respectively. The Stokes shifts for compounds **7** and **8** were 78 and 131 nm, respectively, suggesting that there is a large and fast geometrical conversion between the TPE units as well as between the neighboring aromatic units. These large Stokes shifts typically indicate conformational reorganization in geometry from the pyramidal ground state to a more planar excited state.[14] The PL intensity and fluorescent quantum yield (Φ_F) of **7** and **8** were detected in THF solution (Φ_F for **7** is 0.15%, and Φ_F for **8** is 0.21%).

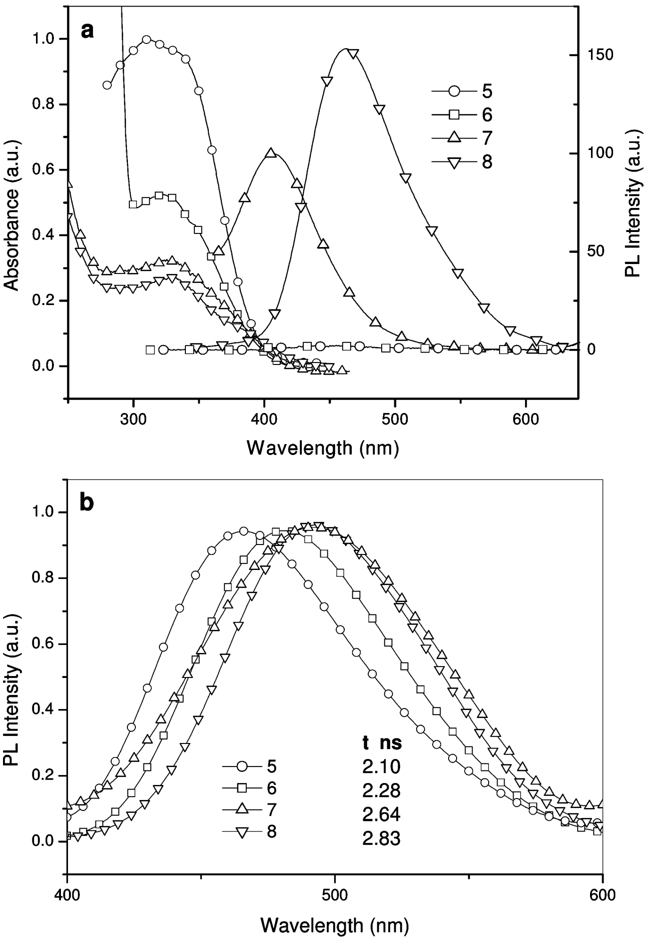

Figure 2. (a) UV−visible absorption and photoluminescence spectra of samples **5**−**8** in THF at room temperature with a concentration of 10 μM. (b) Photoluminescence spectra of solid films of **5**−**8** (obtained by spin-coating a solution with a concentration of 100 μM).

Unlike the solution PL spectra, the solid films of all the four samples emitted light when they were exposed to UV irradiation. The PL spectra of the solid films of **5**−**8** are shown in Figure 2b, and the corresponding emission peaks and Φ_F are 469, 480, 486, and 490 nm, and 25.8, 30.2, 44.0, and 47.8%, respectively. Comparing the samples in solution and in solid films, we observe two obvious differences. One difference is in the fluorescence intensity. Samples **5** and **6** emitted light in the solid state but were almost nonemissive in solution. However, the change in fluorescence intensity for samples **7** and **8** with more steric hindrance was not so obvious. This phenomenon can probably be explained by the existence of a nonradiative decay pathway of the singlet excited state. It is known that rotational energy relaxation can nonradiatively deactivate excited species.[15] In solutions at room temperature, phenyl rings against the ethylene core of samples **5** and **6** have enough space for intramolecular motions [motions include rotation (e.g., $C_{Ph}{-}C{=}$ torsion) and vibration (e.g., $C_{Ph}{-}C{=}$ stretching and bending); the space structures of samples **5** and **6** can be found in the Supporting Information]. This type of steric hindrance will effectively deactivated the excited states by the rotation, thus making the molecules nonemissive. However, for samples **7** and **8**, which have a sterically crowded structure (see Supporting Information

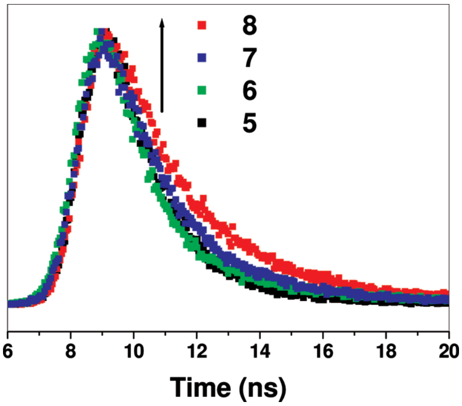

Figure 3. Fluorescence decay curves of solid film of samples **5**−**8**.

Figures S30 and S31), this nonradiative decay pathway of its singlet excited state is blocked. Therefore, **7** and **8** can emit light in solution with fluorescence intensities depending on the extent of steric hindrance in the molecule. In the solid aggregate state, interactions involved in the crystal packing may restrict the intramolecular rotations, which may block the nonradiative channel and stop the radiative decay, thus making the film sample luminescent. This is why samples **5** and **6**, as derivatives of TPE, show AIE. It is also possible that samples **7** and **8** show reduced AIE (in other words, samples **7** and **8** exhibit AIEE) by increasing the steric hindrance of the structure.

Another obvious difference in solid state PL of the compounds is the shift of emission wavelength. Extending the length of conjugated chains results in a red shift of fluorescence spectra. However, the difference in the emission wavelength of the solid films of **5**−**8** decreases steadily (for **5** to **6**, 11 nm; for **6** to **7**, 6 nm; for **7** to **8**, 4 nm). If we take the changes in steric hindrance into account, a possible explanation is that the red shift usually observed by extending the conjugated chain is counteracted by the blue shift caused by the increase in steric hindrance. The effect of steric hindrance on the emission wavelength has also been proven by the characterization of the fluorescence lifetimes (τ) of the solid films, as shown in Figure 3. Sample **5**, which is inclined to crystallize with less steric hindrance, has more intramolecular or intermolecular interactions, thus resulting in a short fluorescence lifetime of 2.10 ns. Following the above concept, it is clear that the τ increases from 2.28 to 2.64 to 2.83 ns for **6**, **7**, and **8**, respectively, due to the increased steric hindrance within the sample.

To provide further evidence for the above hypothesis, the dependence of the Φ_F of **5**−**8** on the solvent composition of the acetonitrile/water mixture is shown in Figure 4. In the mixtures with a water content of less than 50%, the Φ_F for **5** and **6** are very small (0.026% for **5** and 0.032% for **6**) because their molecules are dissolved in the solvent mixtures. Φ_F starts to increase at a water content of >50%, suggesting that the molecules begin to aggregate in the solvent mixture with this composition. The Φ_F values of both **5** and **6** continuously increase with an increase in the water content, reaching a maximum of 6.7% and 8.8%, respectively, at water content of 90%. This is an increase in Φ_F of more than 250-fold for both **5** and **6** over their respective dilute acetonitrile solutions under the same measurement conditions. Further increasing the water content to 95% results in a decrease in Φ_F due to a morphological change, as suggested by Tang.[6d] The emission properties of samples **5** and **6** clearly proves that they exhibit AIE. Compared to **5** and **6**, derivatives **7** and **8** show little AIE, instead exhibiting AIEE. The acetonitrile solutions of **7** and **8** are luminescent (Φ_F for 7 is 5.8%, Φ_F for 8 is 9.5%), because the intramolecular rotations are more restricted for more sterically hindered groups. The Φ_F of **7** and **8** display different trends to those of **5** and **6**. At a water content of 0−70%, the Φ_F values of **7** and **8** gradually increase. When the water content is increased to 80%, the Φ_F values for **7** and **8** reach a maximum of 16.1% and 20.4%, respectively, which are 2.8 and 2.1 times higher than the Φ_F vlues of their respective acetonitrile solutions. At very high water contents, Φ_F decreases a little.

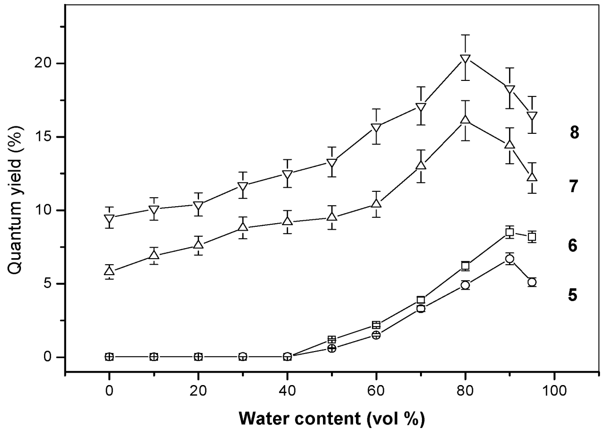

Figure 4. Dependence of quantum yield on the water content in acetonitrile/water mixtures of samples **5**−**8**. Sample concentration: **5** and **6**, 10 μM; **7** and **8**, 1 μM. Excitation wavelength: 350 nm.

Electrochemical Properties. Cyclic voltammetry (CV) measurements of **5**−**8** films coated on a glassy carbon electrode (~0.08 cm^2) were performed in an electrolyte of 0.1 M tetrabutylammonium hexafluorophosphate (TBAPF$_6$) in acetonitrile using ferrocene (4.8 eV below vacuum) as the internal standard at a scan rate of 100 mV/s at room temperature under the protection of argon. A Pt wire was used as the counter electrode, and an Ag/AgNO$_3$ electrode was used as the reference electrode. The corresponding data are summarized in Table 1. On the basis of the onset potentials of the oxidation (0.85 to 0.70 V) and reduction (−2.03 to −1.73 V), we estimated the HOMO and LUMO energy levels of **5**−**8** to be 5.60, 5.53, 5.47, 5.45 eV and 2.72, 2.65, 2.57, 2.46 eV, respectively, with regard

TABLE 1: Electrochemical Properties of Samples 5−8[a,b]

			HOMO (eV)		LUMO (eV)		E_g (eV)	
compound	$E_{\text{onset}}^{\text{ox}}$ (V)	$E_{\text{onset}}^{\text{red}}$ (V)	exptl	calc	exptl	calc	exptl	calc
5	0.85	−2.03	−5.60	−4.731	−2.72	−2.454	2.88	2.277
6	0.78	−1.92.	−5.53	−4.625	−2.65	−2.589	2.70	2.036
7	0.72	−1.84	−5.47	−4.591	−2.57	−2.556	2.56	2.035
8	0.70	−1.73	−5.45	−4.564	−2.46	−2.562	2.43	2.002

[a] Determined from cyclic voltammetry in acetonitrile for oxidation potentials and in THF for reduction potentials (0.1 M n-Bu$_4$N$^+$PF$_6^-$ as a supporting electrolyte) using Ag/Ag+ (0.01 M) as a reference electrode at a scan rate of 100 mV/s. [b] HOMO and LUMO levels were determined using the following equations: HOMO/LUMO = $-e(E_{\text{onset}} - 0.0468\text{ V}) - 4.8$ eV, where the value 0.0468 V is for FOC vs Ag/Ag$^+$.

to the energy level of ferrocene. The band gaps of samples **5−8** are 2.88, 2.70, 2.56, and 2.43 eV, which have the same trends with the calculated data in Table S2 (Supporting Information). DFT calculations show that, for the TPEs, the lowest unoccupied molecular orbital (LUMO) is stabilized by a bonding interaction between the π-system and the double bond (Figure S27−S31 in Supporting Information). The DFT calculations also reveal that the HOMO diminishes significantly as the oligomer length increases (from **5** to **8**).

Conclusion

In summary, we have studied aggregation emission properties of oligomers based on tetraphenylethylene in solution and aggregate states. Due to the rigidity and steric hindrance in molecular structure enhanced regularly, UV−visible absorption and PL spectra of **5−8** reveal the transition from AIE to AIEE behavior. Lifetime measurements reveal that the excited species of samples become longer-lived in the aggregates. All samples **5−8** become more emissive when their chains are induced to aggregate by adding water into their acetonitrile solutions. Cyclic voltammetry measurements and theoretical calculations also support the bad gap results. The conformational simulations also suggest that the origin of transition from AIE to AIEE behavior is the restricted intramolecular rotations of the aromatic rings in samples.

Acknowledgment. This paper was inspired by Prof. Ben Zhong Tang' s lecture in Fudan 2008. This work was financially supported by the National Natural Science Foundation of China (20974022, 20704009, 20774019, 50873027), the Opening Project of Key Lab for Special Functional Materials, Henan University (0701).

Supporting Information Available: Crystal date (cif file). Figures showing the ^{1}H NMR, ^{13}C NMR, and MALDI-TOF of compounds **1−8**, ^{1}H−^{1}H COSY of compound **2**, byproducts in the synthesis of TPE derivatives, and frontier orbitals. Tables of reaction data and theoretical calculations. This material is available free of charge via the Internet at http://pubs.acs.org.

References and Notes

(1) (a) Schultz, A.; Laschat, S.; Diele, S.; Nimtz, M. *Eur. J. Org. Chem.* **2003**, *15*, 2829–2839. (b) Mallory, F. B.; Mallory, C. W. *Org. React.* **1984**, *30*, 1–456. (c) Oliveira, R. P.; Martin, S. E. *J. Org. Chem.* **2000**, *65*, 7010–7019. (d) Eshdat, L.; Ayalon, A.; Beust, R.; Shenhar, R.; Rabinovitz, M. *J. Am. Chem. Soc.* **2000**, *122*, 12637–12645. (e) Tellenbroecker, J.; Kuck, D. *Angew. Chem.* **1999**, *111*, 1000–1004. (f) Niu, C.; Petterson, T.; Miller, M. J. *J. Org. Chem.* **1996**, *61*, 1014–1022.

(2) (a) Wang, G.; Janssens, K.; Van Oosterwijck, C.; Yakimansky, A.; Van Beylen, M. *Polymer* **2005**, *46*, 295–302. (b) Wolf, M. O.; Fox, H. H.; Fox, M. A. *J. Org. Chem.* **1996**, *61*, 287–294.

(3) Sengupta, S. *Synlett* **2004**, *7*, 1191–1194.

(4) (a) Ito, A.; Nakano, Y.; Kato, T.; Tanaka, K. *Chem. Commun.* **2005**, *3*, 403–405. (b) Mori, T.; Inoue, Y. *J. Phys. Chem. A* **2005**, *109*, 2728–2740.

(5) Liu, L.; Zhang, G.; Xiang, J.; Zhang, D.; Zhu, D. *Org. Lett.* **2008**, *10*, 4581–4584.

(6) (a) Luo, J.; Xie, Z.; Lam, J.; Cheng, L.; Chen, H.; Qiu, C.; Kwok, H. S.; Zhan, X.; Liu, Y.; Zhu, D.; Tang, B. Z. *Chem. Commun.* **2001**, *18*, 1740–1741. (b) Chen, J.; Law, C. W.; Lam, J.; Dong, Y.; Lo, S.; Williams, I. D.; Zhu, D.; Tang, B. Z. *Chem. Mater.* **2003**, *15*, 1535–1546. (c) Tong, H.; Hong, Y.; Dong, Y. Q.; Häussler, M.; Lam, J.; Li, Z.; Guo, Z. f.; Guo, Z. H.; Tang, B. Z. *Chem. Commun.* **2006**, *35*, 3705–3707. (d) Tong, H.; Dong, Y.; Häussler, M.; Lam, J.; Sung, H. H.; Williams, I. D.; Tang, B. Z. *Chem. Commun.* **2006**, *10*, 1133–1135.

(7) (a) Yu, G.; Yin, S. W.; Liu, Y. Q.; Chen, J. S.; Xu, X. J.; Sun, X. B.; Ma, D. G.; Zhan, X. W.; Peng, Q.; Shuai, Z. G.; Tang, B. Z.; Zhu, D. B.; Fang, W. H.; Luo, Y. *J. Am. Chem. Soc.* **2005**, *127*, 6335–6346. (b) Lee, S. H.; Jang, B. B.; Kafafi, Z. H. *J. Am. Chem. Soc.* **2005**, *127*, 9071–9078. (c) Han, M.; Hara, M. *J. Am. Chem. Soc.* **2005**, *127*, 10951–10955. (d) Kim, S.; Zheng, Q. D.; He, G. S.; Bharali, D. J.; Pudavar, H. E.; Baev, A.; Prasad, P. N. *Adv. Funct. Mater.* **2006**, *16*, 2317–2323. (e) An, B. K.; Kwon, S. K.; Jung, S. D.; Park, S. Y. *J. Am. Chem. Soc.* **2002**, *124*, 14410–14415. (f) Zhang, H. Y.; Zhang, Z. L.; Ye, K. Q.; Zhang, J. Y.; Wang, Y. *Adv. Mater.* **2006**, *18*, 2369–2372.

(8) (a) Deans, R.; Kim, J.; Machacek, M. R.; Swager, T. M. *J. Am. Chem. Soc.* **2000**, *122*, 8565–8566. (b) An, B. K.; Kwon, S. K.; Jung, S. D.; Park, S. Y. *J. Am. Chem. Soc.* **2002**, *124*, 14410. (c) Qin, A.; Jim, C. K. W.; Tang, Y.; Lam, J. W. Y.; Liu, J.; Mahtab, F.; Gao, P.; Tang, B. Z. *J. Phys. Chem. B* **2008**, *112*, 9281–9288. (d) Yuan, W. Z.; Qin, A. J.; Lam, J. W. Y.; Sun, J. Z.; Dong, Y. Q.; Häussler, M.; Liu, J. Z.; Xu, H. P.; Zheng, Q.; Tang, B. Z. *Macromolecules* **2007**, *40*, 3159–3166.

(9) Kim, T. H.; Choi, M. S.; Sohn, B. H.; Park, S. Y.; Lyoo, W. S.; Lee, T. S. *Chem. Commun.* **2008**, *20*, 2364–2366.

(10) Zhao, Q.; Li, L.; Li, F.; Yu, M.; Liu, Z.; Yi, T.; Huang, C. *Chem. Commun.* **2008**, 685–687.

(11) (a) McMurry, J. E.; Felming, M. P. *J. Am. Chem. Soc.* **1974**, *96*, 4708–4709. (b) McMurry, J. E. *Acc. Chem. Res.* **1983**, *16*, 405–411.

(12) (a) Mladenova, G.; Chen, L.; Rodriquez, C. F.; Siu, K. W. M.; Johnston, L. J.; Hopkinson, A. C.; Lee-Ruff, E. *J. Org. Chem.* **2001**, *66*, 1109–1114. (b) Rathore, R.; Burns, C. L.; Abdelwahed, S. A. *Org. Lett.* **2004**, *6*, 1689–1692. (c) Banerjee, M.; Emond, S. J.; Lindeman, S. V.; Rathore, R. *J. Org. Chem.* **2007**, *72*, 8054–8061.

(13) Crystal data for **2**: Crystals were grown from CH_2Cl_2. The structure was solved on a Bruker SMART CCD diffractometer using Mo Kα radiation. $C_{40}H_{28}O_2$ ($M_r = 540.62$); monoclinic, space group $C2/c$, $D_c = 1.233$ g cm^{-3}, $a = 16.698(3)$ Å, $b = 10.5516(19)$ Å, $c = 16.706$ (3) Å, $\alpha = 90°$, $\beta = 98.437(2)°$, $\gamma = 90°$, $V = 2911.6(9)$ Å^3, $Z = 4$, $\lambda = 0.710\ 73$ Å, $\mu = 0.075$ mm^{-1}, $T = 296(2)$ K, $R = 0.0264$ for 11 361 observed reflections [$I > 2\sigma I$] and $R_w = 0.0939$ for all 3138 unique reflections. Crystal data for **4**: Crystals were grown from CH_2Cl_2. The structure was solved on a Bruker SMART CCD diffractometer using Mo Kα radiation. $C_{54}H_{36}O_4$ ($M_r = 748.83$); triclinic, space group $P\bar{1}$, $D_c = 1.240$ g cm^{-3}, $a = 10.9819(4)$ Å, $b = 12.2293(4)$ Å, $c = 15.9624$ (7) Å, $\alpha = 78.216(2)°$, $\beta = 85.799(2)°$, $\gamma = 72.961(2)°$, $V = 2006.26(13)$ Å^3, $Z = 2$, $\lambda = 0.710\ 73$Å, $\mu = 0.077$ mm^{-1}, $T = 296(2)$ K, $R = 0.0259$ for 18 656 observed reflections [$I > 2\sigma I$] and $Rw = 0.1139$ for all 8657 unique reflections.

(14) (a) Henssler, J. T.; Zhang, X.; Matzger, A. J. *J. Org. Chem.* **2001**, *66*, 1109–1114. (b) Stott, T. L.; Wolf, M. O. *J. Phys. Chem. B* **2004**, *108*, 18815–18819.

(15) Malkin, J. *Photophysical and Photochemical Properties of Aromatic Compounds*; CRC Press: Boca Raton, FL, 1992.

JP911311J